CrossMark

# A modified intuitionistic fuzzy c-means clustering approach to segment human brain MRI image

**Dhirendra Kumar**[1,2] ⬚ · **Hanuman Verma**[3] ·
**Aparna Mehra**[4] · **R. K. Agrawal**[1]

© Springer Science+Business Media, LLC, part of Springer Nature 2018

**Abstract** Fuzzy c-means (FCM) is one of the prominent method utilized for medical image segmentation. In literature intuitionistic fuzzy c-means (IFCM) is suggested which is based on intuitionistic fuzzy sets (IFSs) theory to handle uncertainty and vagueness associated with real data. The objective function of which is defined using the hesitation degree along with membership degree. However, instead of solving the objective function analytically, the approximate solution is obtained using FCM. In this paper, we have proposed a modified intuitionistic fuzzy c-means algorithm (MIFCM) and solved analytically the objective function of the MIFCM method using Lagrange method of undetermined multiplier. To incorporate hesitation degree, two parametric intuitionistic fuzzy complements namely Sugeno's negation function and Yager's negation function are investigated. The performance of the MIFCM method is compared with three intuitionistic fuzzy clustering methods and the FCM on two publicly available MRI dataset and a synthetic dataset. The performance measures (average segmentation accuracy, dice score, jaccard score, false negative ratio

✉ Dhirendra Kumar
    dhirendra.bhu08@gmail.com

    Hanuman Verma
    hv4231@gmail.com

    Aparna Mehra
    apmehra@maths.iitd.ac.in

    R. K. Agrawal
    rkajnu@gmail.com

[1]   School of Computer & Systems Sciences, Jawaharlal Nehru University, New Delhi, India

[2]   Department of Computer Science, Banasthali Vidyapith, Banasthali, Rajasthan, India

[3]   Acharya Narendra Dev College, Delhi University, New Delhi, India

[4]   Department of Mathematics, Indian Institute of Technology, New Delhi, India

and false positive ratio) are used to compare the performance of the MIFCM method with three variants of intuitionistic fuzzy clustering methods and the FCM. Experimental results demonstrate the superior performance of the MIFCM method over others.

## 1 Introduction

Image segmentation is one of the important phase in image analysis and pattern recognition because of its wide real life applications such as medical image analysis, computer vision, industrial inspections etc.. In last few years, medical image analysis is used for diagnosis of various disease such as Parkinson, Alzheimer, Schizophrenia etc.. For this, many medical imaging modalities, such as Computed Tomography (CT), Magnetic Resonance Imaging (MRI), Positron Emission Tomography (PET), Mammogram, X-rays, Ultrasound etc., are being utilized to analyze the human organs and further these images are used to examine the diseases for clinical studies.

Among these modalities, MRI is a popular imaging modality as it is non-invasive and does not have any harmful effects on human tissues. Segmentation of brain MRI into various brain tissues namely white matter (WM), gray matter (GM), cerebrospinal fluid (CSF) is important for diagnosis of various diseases. However, manual segmentation of brain MRI image is not only time consuming but also difficult task due to complicated structure and absence of well-defined boundary between different brain tissues. Hence, to reduce the time and assist the radiologists for better analysis of MRI images, many segmentation approaches have been proposed in literature such as level set [1, 21, 33], graph cut [9], region growing [27] and clustering [4, 5, 11, 14, 17–19, 23, 25, 26, 34]. Among these segmentation techniques, clustering based on fuzzy set theory [38] known as fuzzy c-means (FCM) [6] and its variants are found to be better in comparison to conventional hard clustering algorithm. The advantage of the FCM and its variants is that a given data point is assigned to more than one cluster with membership grade in the interval of [0, 1]. The degree of membership of a data point to a cluster is inversely proportional to the distance of data point from the cluster centroid. However, in real world applications, there is always an uncertainty associated with the localization of a data point as it is subject to uncertainty owing to its imprecise measurement and noise. Due to this, an uncertainty arises in the computation of membership of a data point to a given cluster and centroid [24]. To handle uncertainty in the localization of a data point, Atanassov proposed intuitionistic fuzzy sets (IFSs) theory. IFSs are extension of fuzzy sets which can deal with uncertainty and vagueness associated with real data as it takes advantage of non-membership degree and hesitation degree along with membership degree for representing the real data [28]. Recently, IFSs theory based clustering is utilized for segmentation of images [2, 3, 8, 15, 35]. The intuitionistic fuzzy based clustering is more accurate, robust to noise and converges faster in comparison to conventional FCM [15].

The research work [8] used IFSs theory for medical image segmentation which utilizes Yager's negation function for calculating non-membership degree and hesitation degree of a data point to a given cluster. The author defined an objective function which incorporated the

hesitation degree along with membership degree. However, instead of solving the objective function analytically, the approximate solution is obtained. To obtain the centroid of the clusters, the membership value in the equation of centroid of the FCM algorithm is simply replaced with the sum of membership and hesitation value in the research work [8]. Hence, the cluster centroids and the membership so obtained are not reasonable.

In this work, we have solved analytically the objective function of modified intuitionistic fuzzy c-means algorithm (MIFCM) using Lagrange method of undetermined multiplier. To incorporate hesitation degree, two parametric intuitionistic fuzzy complements namely Sugeno's negation function and Yager's negation function is utilized. The performance of the MIFCM method is compared with three intuitionistic fuzzy clustering methods [8, 29, 35] and the FCM on two publicly available MRI datasets and a synthetic dataset. The performance measures used for comparison are: average segmentation accuracy (*ASA*), dice score (*DS*), jaccard score (*JS*), false negative ratio (*FNR*) and false positive ratio (*FPR*) [32]. Contributions of this research work can be summarized as follows:

–   The hesitation is properly incorporated in modified intuitionistic fuzzy c-means algorithm in contrast to the research work [8].
–   Two negation functions are investigated namely Sugeno's negation function and Yager's negation function for incorporating hesitation.

The paper is organized as follows. In Section 2, related work is described. The preliminaries on the fuzzy set and intuitionistic fuzzy set are described in Section 3. In Section 4, the proposed method is included. Details of datasets used for experiment and results are given in Section 5. Finally the conclusion is drawn in Section 6.

## 2 Related work

The fuzzy c-means clustering (FCM), introduced by Bezdek, is a popular clustering algorithm which works on the idea of belongingness of a given data point to more than one cluster [6]. After clustering, all the obtained $c$ clusters are represented as fuzzy sets $F = \{F_1, F_2, F_3, \ldots, F_c\}$ defined on the data points $X = \{x_1, x_2, x_3, \ldots, x_n\}$. However, the non-membership degree for a data point to a given cluster is just equal to 1 minus membership degree which may not always be the case with real data [2, 3]. In order to incorporate more information about data, intuitionistic fuzzy set was proposed by Atanassov [2]. To cluster the intuitionistic fuzzy sets, Intuitionistic fuzzy c-means (IFCM) [35] is proposed which utilizes intuitionistic fuzzy distance measure [28]. In the research work [8], a novel intuitionistic fuzzy c-means clustering algorithm is proposed using the intuitionistic fuzzy set theory for calculating the hesitation degree that arises while defining the membership function. Recently, another variant of IFCM was proposed to segment the MRI images, termed as neighborhood intuitionistic fuzzy c-means clustering algorithm with genetic algorithm (NIFCMGA), which exploits neighborhood membership to reduced the effect of noise/outlier [14]. In the research work [29], possibilistic intuitionistic fuzzy c-means (PIFCM) algorithm was proposed for clustering intuitionistic fuzzy sets which includes the advantages of the possibilistic c-means (PCM) [20] and IFCM. Another variant of IFCM algorithm, known as improved intuitionistic fuzzy c-means (IIFCM) which utilizes the local spatial information in an intuitionistic fuzzy way for segmenting the brain MRI images was proposed in the research work [30].

# 3 Preliminaries

The description of notations used in this work and related definition is described here in this section.

**Definition 1** Fuzzy set: A Fuzzy set is a set in which each member element will have the fractional membership via a membership function $\mu_A : X \rightarrow [0, 1]$ which give its degree of belongingness [38]. If $A$ is a fuzzy set defined over a set $X$, it can be represented as:

$$A = \{(x, \mu_A(x)) : x \in X\} \tag{1}$$

**Definition 2** Intuitionistic fuzzy set: A Intuitionistic fuzzy set $B$, is an extension of fuzzy set over $X$ which is represented as [2]:

$$B = \{(x, \mu_B(x), \nu_B(x)) : x \in X \ and \ 0 \leq \mu_B(x) + \nu_B(x) \leq 1\} \tag{2}$$

where $\mu_B : X \rightarrow [0, 1]$, $\nu_B : X \rightarrow [0, 1]$ are membership and non-membership functions of an element x in the set $B$. The IFS B is reduced to FS B when $\mu_B(x) + \nu_B(x) = 1$ for all $x$ in $B$.

**Definition 3** Hesitation: Hesitation degree arises due to lack of knowledge in defining the membership function corresponding to the elements in universe in IFS $B$ [2]. Hesitation degree $\pi_B(x)$ of an elements $x$ in IFS $B$ can be obtained as [2]:

$$\pi_B(x) = 1 - \mu_B(x) - \nu_B(x) \tag{3}$$

where $\mu_B : X \rightarrow [0, 1]$, $\nu_B : X \rightarrow [0, 1]$ are respectively membership and non-membership functions of an element x in the IFS $B$. This hesitation degree $\pi_B(x)$ forces the membership value to lie in the interval $[\mu_B(x), \mu_B(x) + \pi_B(x)]$.

**Definition 4** A continuous function $\phi(\mu)$ can be called intuitionistic fuzzy generator [7] if:

$$\phi(\mu) \leq (1 - \mu) \ for \ all \ \mu \in [0, 1] \ and \ \phi(0) \leq 1 \ and \ \phi(1) \leq 0 \tag{4}$$

Using this generating function, one can define the fuzzy complement function or negation function $N(\mu)$ as [7]:

$$N(\mu) = g^{-1}(g(1) - g(\mu)) \tag{5}$$

where $g : [0, 1] \rightarrow [0, 1]$ is a intuitionistic fuzzy generator and $g(.)$ is an increasing function.

**Definition 5** A Sugeno class can be generated by using the following generating function [22]:

$$g(\mu) = \frac{1}{\lambda} \log(1 + \lambda\mu) \tag{6}$$

Using the above definition of negation function, the non-membership values for a given membership values for any element $x$ in IFS $B$ can be defined as follows:

$$\nu_B(x) = N(\mu_B(x)) = \frac{1 - \mu_B(x)}{1 + \lambda\mu_B(x)}, \ \lambda > 0 \tag{7}$$

**Definition 6** A Yager class can be generated by using the following generating function [36, 37]:

$$g(x) = x^{\alpha} \tag{8}$$

The negation function or non-membership values using this generating function is calculated as:

$$v_B(x) = N(\mu_B(x)) = (1 - \mu_B(x)^\alpha)^{\frac{1}{\alpha}}, \ \alpha > 0 \tag{9}$$

**Definition 7** intuitionistic fuzzy distance between the elements $\mathbf{x}_i^{IFS} = \langle \mu(x_i), v(x_i), \pi(x_i) \rangle$ and $\mathbf{x}_j^{IFS} = \langle \mu(x_j), v(x_j), \pi(x_j) \rangle$ of an IFS $X^{IFS}$ is defined as [28]:

$$\|\mathbf{x}_i^{IFS} - \mathbf{x}_j^{IFS}\| = \sqrt{\frac{1}{2}((\mu(x_i) - \mu(x_j))^2 + (v(x_i) - v(x_j))^2 + (\pi(x_i) - \pi(x_j))^2)} \tag{10}$$

### 3.1 Intuitionistic fuzzy image representation

Intuitionistic fuzzy generator defined above is used to construct the intuitionistic fuzzy image for clustering [31]. Let $X$ be the set of voxel intensity with intensity value $x_j$ at $j^{th}$ pixel where $j \in 1, 2, \ldots N$ and $N$ is total number of pixels. These voxel intensity values are normalized to [0 1] for creating the IFSs corresponding to a given image. Let $X^{IFS}$ be the IFS defined on set $X$ with $j^{th}$ element $\mathbf{x}_j^{IFS}$ as IFS element $\langle \mu_X(x_j), v_X(x_j), \pi_X(x_j) \rangle$ corresponding to $j^{th}$ voxel with intensity value $x_j$, where $\mu_X(x_j)$ is the normalized intensity value and $v_X(x_j)$ is calculated using one of the negation functions described above. $\mathbf{U}$ represents the fuzzy partition matrix defined as $\mathbf{U} = \{\mu_i(x_j) : \mu_i(x_j) \in [0, 1]; \sum_{i=1}^{c} \mu_i(x_j) = 1; \ \forall j \in \{1, 2, \ldots N\} \ and \ i \in \{1, 2, \ldots c\}\}$ which divides the image into $c$ equivalence classes with each class $i$ representing the membership value $\mu_i(x_j)$ of $j^{th}$ voxel $\forall j \in 1, 2, \ldots N$. $v_i(x_j)$ and $\pi_i(x_j)$ represent the non-membership values and hesitation degree for $j^{th}$ voxel in $i^{th}$ class or cluster respectively. For simplicity, in rest of the paper, $\mu_i(x_j)$, $v_i(x_j)$ and $\pi_i(x_j)$ are denoted as $\mu_{ij}$, $v_{ij}$ and $\pi_{ij}$ respectively.

### 3.2 Fuzzy c-means

Fuzzy clustering allows each data point to belong to more than one cluster. Let $\mathbf{X}$ be a set of feature vectors with total N elements and $c$ represents number of clusters. The FCM algorithm is formulated as the minimization of objective function $J_m(\mathbf{U}, \mathbf{V} : \mathbf{X})$ given by:

$$\min J_m(\mathbf{U}, \mathbf{V} : \mathbf{X}) = \sum_{i=1}^{c} \sum_{j=1}^{N} \mu_{ij}^m \|x_j - v_i\|^2 \tag{11}$$

$$subject \ to \ \sum_{i=1}^{c} \mu_{ij} = 1, \ 1 \le j \le N \tag{12}$$

where $m \in (1, \text{inf})$ is fuzzifier constant, $\mathbf{U} = \{\mu_{ij}\}_{c \times N}$ is fuzzy partition matrix over the set $\mathbf{X}$ into $c$ equivalence classes with the cluster prototype $\mathbf{V} = \{v_i\}$. $\mu_{ij}$ and $v_i$ represents the membership of $j^{th}$ element to the $i^{th}$ cluster and cluster center of $i^{th}$ class respectively. The solution of (11) is obtained using Lagrange method of undetermined multiplier, which are given as:

$$\mu_{ij} = \frac{(\|x_j - v_i\|^2)^{\frac{-1}{(m-1)}}}{\sum_{k=1}^{c} (\|x_j - v_k\|^2)^{\frac{-1}{(m-1)}}} \tag{13}$$

$$v_i = \frac{\sum_{j=1}^{N} \mu_{ij}^m x_j}{\sum_{j=1}^{N} \mu_{ij}^m}, \ 1 \le i \le c \tag{14}$$

## 4 Modified intuitionistic fuzzy c-means algorithm

The research work [35] used intuitionistic fuzzy distance in the objective function for clustering. However, they have not included hesitation degree in the objective function. On the other hand, the research work [8] utilized hesitation degree in the objective function for clustering. Instead of the intuistionistic fuzzy distance, Euclidean distance is used in this work. However, instead of solving the objective function analytically; the approximate solution is obtained using FCM in the research work [8]. Hence, the cluster centroids and the membership so obtained are not reasonable. In order to overcome the shortcomings of the research works [8, 35], we have used both hesitation degree and intuitionistic fuzzy distance in the modified objective function. We called this method as modified intuitionistic fuzzy c-means algorithm (MIFCM). The optimization problem for the MIFCM method is defined by incorporating the hesitation degree $\pi_{ij}$ which is another kind of uncertainty arises while defining the membership degree $\mu_{ij}$ as described in Definition 3 and IFS distance measure (Definition 7). The optimization problem to be solved for clustering the data using the MIFCM method can be given as:

$$\min J_m(\mathbf{U}, \mathbf{V} : \mathbf{X}) = \sum_{i=1}^{c} \sum_{j=1}^{N} (\mu_{ij} + \pi_{ij})^m \|\mathbf{x}_j^{IFS} - \mathbf{v}_i^{IFS}\|^2 \tag{15}$$

$$subject\ to\ \sum_{i=1}^{c} \mu_{ij} = 1,\ 1 \le j \le N \tag{16}$$

**Case I** Using Sugeno's negation function

Utilizing the Sugeno's negation function, as defined in Definitions 3 and 5, we can write the sum of $\mu_{ij}$ and $\pi_{ij}$ as follows:

$$\mu_{ij} + \pi_{ij} = \frac{(\lambda + 1)\mu_{ij}}{1 + \lambda\mu_{ij}} \tag{17}$$

Hence the optimization problem (15) can be rewritten as,

$$\min J_m(\mathbf{U}, \mathbf{V} : \mathbf{X}, \lambda) = \sum_{i=1}^{c} \sum_{j=1}^{N} \left(\frac{(\lambda + 1)\mu_{ij}}{1 + \lambda\mu_{ij}}\right)^m \|\mathbf{x}_j^{IFS} - \mathbf{v}_i^{IFS}\|^2 \tag{18}$$

$$subject\ to\ \sum_{i=1}^{c} \mu_{ij} = 1,\ 1 \le j \le N \tag{19}$$

After solving the above equation using Lagrange method of undetermined multiplier, the membership value $\mu_{ij}$ and cluster center $\mathbf{v}_i^{IFS} = \langle \mu_V(v_i), \nu_V(v_i), \pi_V(v_i) \rangle$ can be given as:

$$\mu_{ij} = \frac{(1 + \lambda\mu_{ij})^{\frac{m+1}{m-1}} (\|\mathbf{x}_j^{IFS} - \mathbf{v}_i^{IFS}\|)^{\frac{-2}{m-1}}}{\sum_{k=1}^{c} (1 + \lambda u_{kj})^{\frac{m+1}{m-1}} (\|\mathbf{x}_j^{IFS} - \mathbf{v}_k^{IFS}\|)^{\frac{-2}{m-1}}} \tag{20}$$

$$\mu_V(v_i) = \frac{\sum_{j=1}^{N} \left(\frac{(\lambda+1)\mu_{ij}}{1+\lambda\mu_{ij}}\right)^m \mu_X(x_j)}{\sum_{j=1}^{N} \left(\frac{(\lambda+1)\mu_{ij}}{1+\lambda\mu_{ij}}\right)^m},\ 1 \le i \le c \tag{21}$$

$$v_V(v_i) = \frac{\sum_{j=1}^{N}\left(\frac{(\lambda+1)\mu_{ij}}{1+\lambda\mu_{ij}}\right)^m v_X(x_j)}{\sum_{j=1}^{N}\left(\frac{(\lambda+1)\mu_{ij}}{1+\lambda\mu_{ij}}\right)^m}, \ 1 \le i \le c \tag{22}$$

$$\pi_V(v_i) = \frac{\sum_{j=1}^{N}\left(\frac{(\lambda+1)\mu_{ij}}{1+\lambda\mu_{ij}}\right)^m \pi_X(x_j)}{\sum_{j=1}^{N}\left(\frac{(\lambda+1)\mu_{ij}}{1+\lambda\mu_{ij}}\right)^m}, \ 1 \le i \le c \tag{23}$$

The derivation of the membership value and cluster prototype is included in Appendix A.

**Case II** Using Yagar's negation function

From Definitions 3 and 6 the sum of $\mu_{ij}$ and $\pi_{ij}$ can be rewritten as follows:

$$\mu_{ij} + \pi_{ij} = 1 - (1 - \mu_{ij}^\alpha)^{\frac{1}{\alpha}} \tag{24}$$

The optimization problem (15) (using the Yagar's negation function) is rewritten as:

$$\min J_m(\mathbf{U}, \mathbf{V} : \mathbf{X}, \alpha) = \sum_{i=1}^{c}\sum_{j=1}^{N}[1 - (1 - \mu_{ij}^\alpha)^{\frac{1}{\alpha}}]^m \|\mathbf{x}_j^{IFS} - \mathbf{v}_i^{IFS}\|^2 \tag{25}$$

$$subject\ to\ \sum_{i=1}^{c}\mu_{ij} = 1, \ 1 \le j \le N \tag{26}$$

Solving (25) using Lagrange method of undetermined multiplier, we have

$$\mu_{ij} = \frac{\frac{1}{(t_{ij}d_{ij}^2)^{\frac{1}{\alpha}}}}{\sum_{k=1}^{c}\frac{1}{(t_{kj}d_{kj}^2)^{\frac{1}{\alpha}}}} \tag{27}$$

where $t_{ij}$ and $d_{ij}$ can be given as

$$t_{ij} = [1 - (1 - \mu_{ij}^\alpha)^{\frac{1}{\alpha}}]^{(m-1)}\frac{(1-\mu_{ij}^\alpha)^{\frac{1}{\alpha}}}{\mu_{ij}(1-\mu_{ij}^\alpha)}\ and\ d_{ij} = \|\mathbf{x}_j^{IFS} - \mathbf{v}_i^{IFS}\| \tag{28}$$

the cluster center $\mathbf{v}_i^{IFS} = \langle\mu_V(v_i), v_V(v_i), \pi_V(v_i)\rangle$ can be computed as:

$$\mu_V(v_i) = \frac{\sum_{j=1}^{N}[1 - (1 - \mu_{ij}^\alpha)^{\frac{1}{\alpha}}]^m \mu_X(x_j)}{\sum_{j=1}^{N}[1 - (1 - \mu_{ij}^\alpha)^{\frac{1}{\alpha}}]^m}, \ 1 \le i \le c \tag{29}$$

$$v_V(v_i) = \frac{\sum_{j=1}^{N}[1 - (1 - \mu_{ij}^\alpha)^{\frac{1}{\alpha}}]^m v_X(x_j)}{\sum_{j=1}^{N}[1 - (1 - \mu_{ij}^\alpha)^{\frac{1}{\alpha}}]^m}, \ 1 \le i \le c \tag{30}$$

$$\pi_V(v_i) = \frac{\sum_{j=1}^{N}[1 - (1 - \mu_{ij}^\alpha)^{\frac{1}{\alpha}}]^m \pi_X(x_j)}{\sum_{j=1}^{N}[1 - (1 - \mu_{ij}^\alpha)^{\frac{1}{\alpha}}]^m}, \ 1 \le i \le c \tag{31}$$

Outline of the iterative procedure for finding the solution of the MIFCM method is given in Algorithm 1. The flow diagram of general clustering process based on the MIFCM method is summarized in Fig. 1.

---

**Algorithm 1** Proposed MIFCM algorithm

---

**Require:** Set values for the number of clusters $c$, the degree of fuzziness $m > 1$ , fuzzy negation parameter $\lambda, \alpha$ and the error $\epsilon$.

1: Calculate $\mathbf{x}_j^{IFS} = \langle \mu_X(x_j), \nu_X(x_j), \pi_X(x_j) \rangle \; \forall j \in \{1, 2, \ldots, N\}$ as defined in Section 3.1

2: Initialize the fuzzy partition matrix $\mathbf{U}^{(1)} = \{\mu_{ij}^{(1)}\}_{c \times N} \; \forall i \in \{1, 2, \ldots, c\} \; \& \; \forall j \in \{1, 2, \ldots, N\}$ randomly

3: $k \leftarrow 1$

4: **repeat**

5:     **if** Utilizing Sugeno's negation function **then**

6:         Update the cluster centers $\mathbf{v}_i^{IFS(k)} = \langle \mu_V(x_j)^{(k)}, \nu_V(x_j)^{(k)}, \pi_V(x_j)^{(k)} \rangle$ using (21), (22) and (23)

7:         Calculate the updated fuzzy partition matrix $U^{(k+1)} = \{\mu_{ij}^{(k+1)}\}_{c \times N}$ using (20)

8:     **end if**

9:     **if** Utilizing Yager's negation function **then**

10:         Update the cluster centers $\mathbf{v}_i^{IFS(k)} = \langle \mu_V(x_j)^{(k)}, \nu_V(x_j)^{(k)}, \pi_V(x_j)^{(k)} \rangle$ using (29), (30) and (31)

11:         Calculate the updated fuzzy partition matrix $U^{(k+1)} = \{\mu_{ij}^{(k+1)}\}_{c \times N}$ using (27)

12:     **end if**

13:     $k \leftarrow k + 1$

14: **until** $\|\mathbf{U}^{(k+1)} - \mathbf{U}^{(k)}\| < \epsilon$

15: **return** $\mathbf{v}_i^{IFS}$ the centers of clusters and the membership degrees $\mathbf{U} = \{\mu_{ij}\}_{c \times N}$.

---

It is worth noting from Definitions 3, 5 and 6 that high (low) membership value $\mu_{ij}$ and the low (high) non-membership value $\nu_{ij}$ leads to lesser hesitation value while assigning a given data point $x_j$ to the $i^{th}$ cluster. On the other hand, the case when there is race condition between membership value $\mu_{ij}$ and non-membership value $\nu_{ij}$, hesitation will be high. In this case actual membership value may lie in the interval $[\mu_{ij}, \mu_{ij} + \pi_{ij}]$. The incorporation of the hesitation value will help in determining the actual membership value of a data point to different clusters. Hence, the role of hesitation comes when the data point belongs to boundary region and has almost equal membership value to each cluster. In such a situation, the hesitation value for such data points to each cluster may be high which arises uncertainty as the intensity value corresponding to those voxels contribute to more than one cluster.

Figure 2a shows a cropped MR image from which voxels of $3 \times 3$ window i.e., 9 voxels are selected from the boundary containing three tissues (WM, GM and CSF) and these voxels are indicated using different color in Fig. 2b. The plots of membership vs iteration for these 9 voxels for different brain tissues, obtained using the proposed method (Case I) are shown in Fig. 2c–f. From Fig. 2c–f it can be noted that all the 9 voxels are assigned to correct class. Here, the lower left four voxels assigned to CSF, the upper right two voxels assigned to White Matter and rest of the three voxels assigned to Gray Matter. The voxel intensity values are given as {149, 143, 191; 96, 101, 180; 69, 84, 175}.

## 5 Experimental setup and results

In order to check the efficacy of the proposed method, experiments are performed on a synthetic dataset and two publicly available datasets. The performance is compared with
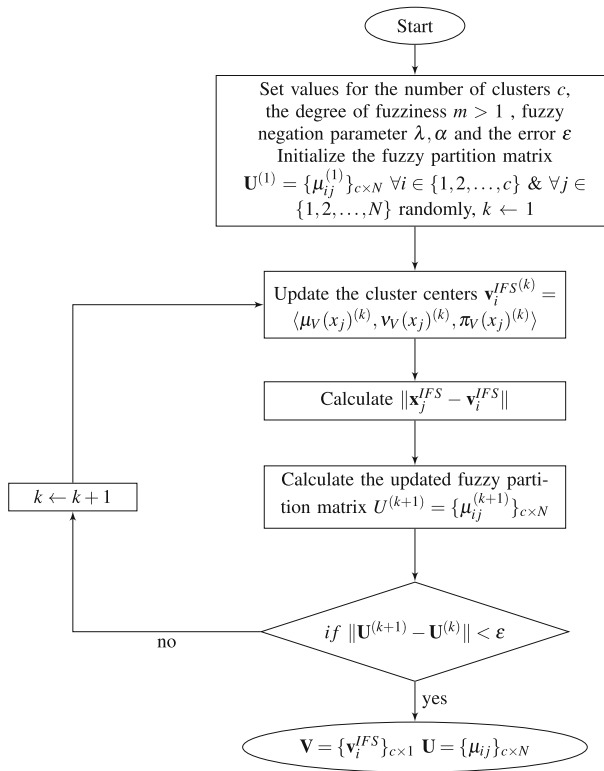
**Fig. 1** Flow diagram of the MIFCM method

conventional FCM, IFCM [8], IFCM [35] and PIFCM [29]. For synthetic dataset, we have used two measures namely partition coefficient and partition entropy for comparison [10, 26]. Partition coefficient (*PC*) can be calculated as follows:

$$PC = \frac{1}{N} \sum_{i=1}^{c} \sum_{j=1}^{N} \mu_{ij}^{m} \tag{32}$$

Partition entropy (*PE*) can be calculated as follows:

$$PE = -\frac{1}{N} \sum_{i=1}^{c} \sum_{j=1}^{N} \mu_{ij} \log \mu_{ij} \tag{33}$$

where $c$ is the number of cluster, $N$ is the total number of datapoints, $\mu_{ij}$ is the membership of $j^{th}$ datapoint in $i^{th}$ cluster and $m$ is the fuzzifier factor.

For other two publicly available datsets, the performance measures used for comparison are average segmentation accuracy (*ASA*), dice score (*DS*), jaccard score (*JS*), false negative

ratio (*FNR*) and false positive ratio (*FPR*) [32]. These performance measures are calculated as:

$$ASA = \sum_{i=1}^{c} \frac{|X_i \cap Y_i|}{\sum_{j=1}^{c}|X_j|} \tag{34}$$

$$DS = \frac{2|X_i \cap Y_i|}{|X_i| + |Y_i|} \tag{35}$$

$$JS = \frac{|X_i \cap Y_i|}{|X_i \cup Y_i|} \tag{36}$$

**Fig. 2** Plot of the membership values for different brain tissues in 3 × 3 window of image for each iteration using the Case I formulation
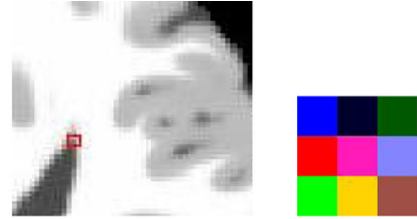


(a) A croped portion of MR image with 3 × 3 window surrounding the tissues

(b) 3 × 3 voxel from the image.
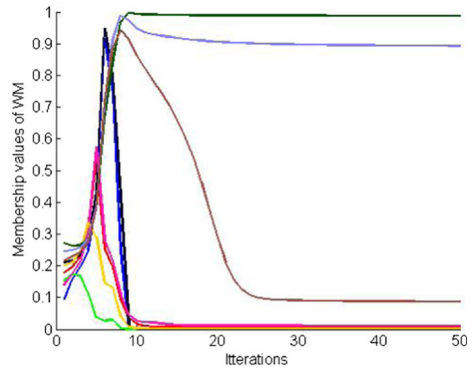


(c) Membership value for White Matter in each iteration.
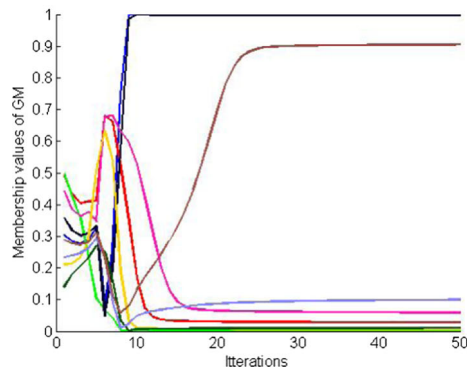


(d) Membership value for Gray Matter in each iteration.
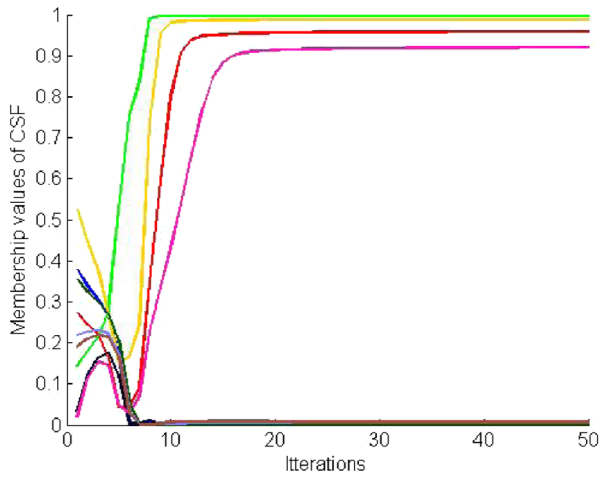
(e) Membership value for CSF in each iteration.
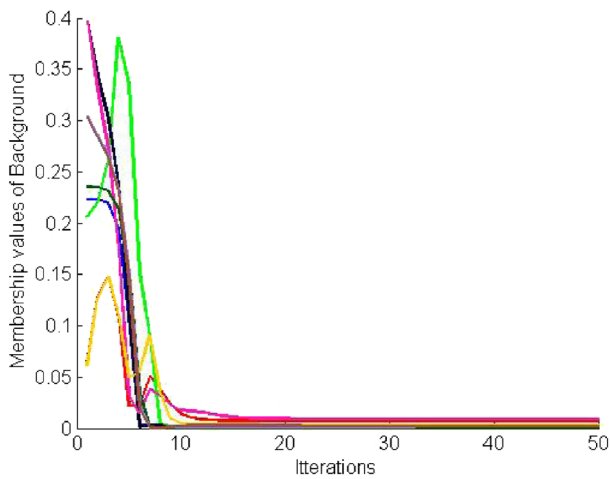


(f) Membership value for Background in each iteration.

**Fig. 2**    (continued)

$$FNR = \frac{|X_i| - |X_i \cap Y_i|}{|X_i|} \tag{37}$$

$$FPR = \frac{|Y_i| - |X_i \cap Y_i|}{|X_i|} \tag{38}$$

where $X_i$ denote the pixels belonging to the manual segmented image (ground truth), $Y_i$ denote the pixels belonging to the experimental segmented image and $|X_i|$ denotes the cardinality of $X_i$.

**Table 1** Value of parameter used for experiment for different datasets

| Algorithms | Parameters | | |
| --- | --- | --- | --- |
| | Synthetic dataset | BrainWeb simulated dataset | IBSR dataset |
| FCM | m = 2 | m = 2 | m = 2 |
| IFCM [8] | $\alpha = 0.95$, m = 2 | $\alpha = 0.95$, m = 2 | $\alpha = 0.9$ m = 2 |
| IFCM [35] | m = 2 | m = 2 | m = 2 |
| PIFCM | m = 2, $\alpha = 1.5$, a = 1, | m = 2, $\alpha = 1.5$, a = 1, | m = 2, $\alpha = 1.5$, a = 1, |
| | b = 1, $\kappa = 0.1$, $\lambda = 1.2$, | b = 1, $\kappa = 0.1$, $\lambda = 1.73$, | b = 1, $\kappa = 0.1$, $\lambda = 1.73$, |
| | $\omega = 1$ | $\omega = 3$ | $\omega = 3$ |
| MIFCM_Sugeno | m = 2, $\lambda = 0.9$ | m = 2, $\lambda = 0.9$ | m = 2, $\lambda = 0.9$ |
| MIFCM_Yager | m = 2, $\alpha = 0.9$ | m = 2, $\alpha = 0.9$ | m = 2, $\alpha = 0.9$ |

### 5.1 Datasets

A new synthetic dataset is generated assuming vertices of the equilateral triangle, whose each side is of length 6 unit, to be the actual cluster centers. Around this assumed cluster centers, we have generated the two dimensional data points inside a circular region of radius 3 unit. We have generated the 300 data points around each of these vertices. Other than this dataset, two publicly available datasets are utilized. BrainWeb simulated MRI brain volumes, a publicly available dataset[1] from the McConnell Brain Imaging Center of the Montreal Neurological Institute, McGill University [11] is used for evaluation of the proposed method. This dataset consist of several simulated T1-weighted brain volume data with different intensity inhomogeneity (0, 20 and 40%) and noise (1, 3, 5, 7 and 9%) of resolution $1 \times 1 \times 1$ mm with $181 \times 217 \times 181$ dimension with the given ground truth for different tissues.

Another publicly available real MRI brain images has been acquired from the Internet Brain Segmentation Repository (IBSR)[2] along with the given ground truth. For all the MRI images, scull striping is done using the brain extraction tool.[3] Table 1 shows the parameter value used for different methods for comparison. The stopping criterion value $\epsilon$ is set to 0.0001 for all the methods.

### 5.2 Experimental results

In this subsection, we have discussed and compared the performance on synthetic dataset and two publicly available datasets using FCM, three different IFCM methods and the MIFCM method.

#### 5.2.1 Results on synthetic dataset

We have compared the MIFCM method with the conventional FCM algorithm and three intuitionistic fuzzy set based IFCM methods on a synthetic dataset. Figure 3a shows the

---

[1]BrainWeb [online], available: http://www.brainweb.bic.mni.mcgill.ca/brainweb.

[2]IBSR [online], available: http://www.cma.mgh.harvard.edu/ibsr/

[3]Brain Extraction Tool (BET) [online], available: http://www.fmrib.ox.ac.uk/fsl/.

(a) Original data point

(b) Clusters using FCM clustering
algorithm

(c) Clusters using IFCM([8]) clustering
algorithm

(d) Clusters using IFCM([35]) clustering
algorithm

(e) Clusters using PIFCM clustering
algorithm

(f) Clusters using the MIFCM_Sugeno
algorithm

(g) Clusters using the MIFCM_Yager
algorithm
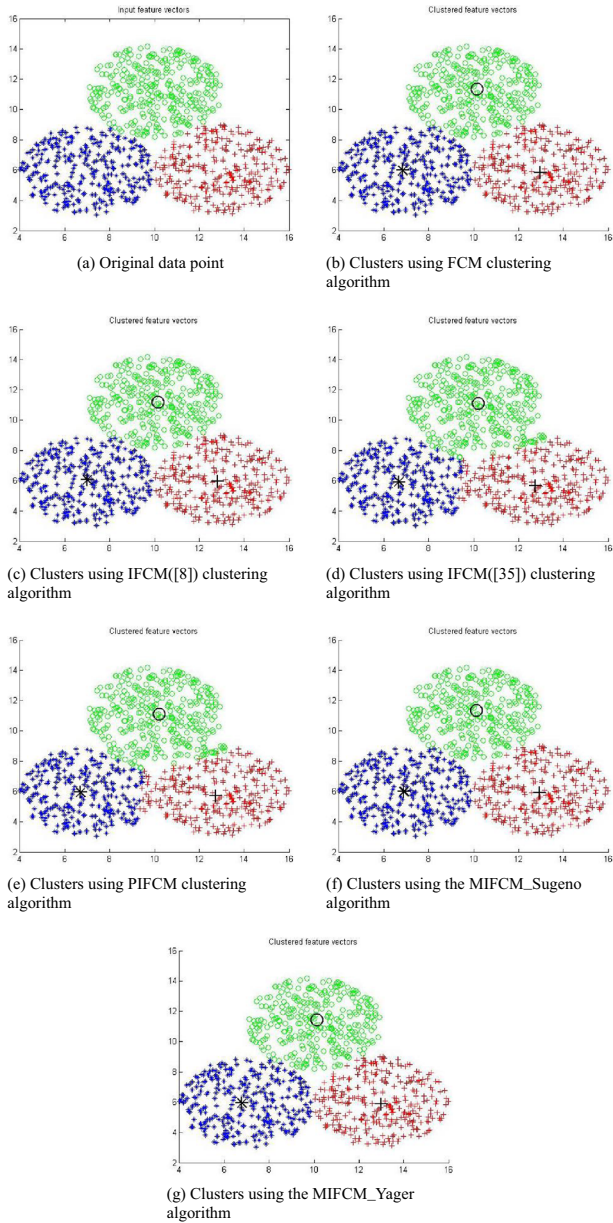
**Fig. 3** Results obtained from various IFCM based algorithms on triangle dataset

original datapoint of this dataset and Fig. 3b–g indicate the qualitative results obtained from
the conventional FCM, three IFCM methods and proposed method respectively. Table 2
shows the partition coefficient (*PC*) and partition entropy (*PE*) obtained for conventional
FCM, different IFCM methods and proposed method. From Table 2, it can be noted that the
proposed method achieved the highest partition coefficient *PC* value and lowest clustering

**Table 2** Comparison in terms of cluster validity measures for synthetic data

|     | FCM  | IFCM [8] | IFCM [35] | PIFCM | MIFCM_Sugeno | MIFCM_Yager |
|-----|------|----------|-----------|-------|--------------|-------------|
| PC  | 0.69 | 0.68     | 0.67      | 0.83  | 0.90         | 0.89        |
| PE  | 0.57 | 0.59     | 0.60      | 0.33  | 0.22         | 0.21        |

entropy *PE*, which indicates the superior clustering capability of the proposed method in comparison to other methods.

### 5.2.2 Results on simulated brain images

We have considered the optimal parameter while comparing various IFCM methods, conventional FCM with the proposed method on the simulated brain images. Table 3 shows the average segmentation accuracy for synthetic brain MR images with 0, 20 and 40% INU and with 7 and 9% noise level for axial slice 90. From Table 3, it can be observed that the MIFCM method using Sugeno's and Yager's negation function, on an average outperformed the existing methods. Tables 4, 5, 6 and 7 indicate comparison of the proposed method with other methods in terms of the performance measures : *DS*, *JS*, *FNR* and *FPR* for WM, GM and CSF. Table 8 shows the comparison of computation time taken for BrainWeb MRI images over 30 runs for different methods (The best results among different methods achieved are shown in bold). It can be noted that the proposed method with Yager's negation function is computationally expensive in comparison to Sugeno's negation function. Though the computation time of the proposed method with Sugeno's negation function is higher with other state of the art methods, however the performance of proposed method with Sugeno's negation function is better in comparison to FCM, IFCM [8], IFCM [35] and PIFCM (see Table 3).

### 5.2.3 Results on real brain images

We have compared the MIFCM_Sugeno, MIFCM_Yager with FCM and three different IFCM methods on 2D axial slices of T1-weighted real brain images from IBSR where ground truth are given. Table 9 shows the average segmentation accuracy for GM on 14 (case 100_23, case 110_3, case 111_2, case 112_2, case 11_3, case 12_3, case 13_3, case 17_3, case 191_3, case 1_24, case 202_3, case 205_3, case 7_8, case 8_4) IBSR real brain MRI images on slice 134 for the proposed method and the other existing methods. From Table 9, it can be noted that average segmentation performance measure *ASA* on individual images and overall average performance of the proposed method is better than the other

**Table 3** Average segmentation accuracy for BrainWeb simulated MRI

| INU | Noise | FCM    | IFCM [8] | IFCM [35]  | PIFCM  | MIFCM_Sugeno | MIFCM_Yager |
|-----|-------|--------|----------|------------|--------|--------------|-------------|
| 0   | 7     | 0.8689 | 0.8677   | **0.8776** | 0.8737 | 0.8771       | 0.8698      |
|     | 9     | 0.8160 | 0.8121   | 0.8398     | 0.8329 | **0.8401**   | 0.8207      |
| 20  | 7     | 0.8775 | 0.8765   | 0.8835     | 0.8824 | **0.8846**   | 0.8782      |
|     | 9     | 0.8180 | 0.8155   | 0.8405     | 0.8319 | **0.8417**   | 0.8204      |
| 40  | 7     | 0.8562 | 0.8555   | **0.8697** | 0.8653 | **0.8697**   | 0.8573      |
|     | 9     | 0.8087 | 0.8060   | 0.8309     | 0.8268 | **0.8311**   | 0.8124      |

**Table 4** Dice Score for BrainWeb simulated MRI

|     | INU | Noise | FCM | IFCM [8] | IFCM [35] | PIFCM | MIFCM_Sugeno | MIFCM_Yager |
|-----|-----|-------|-----|----------|-----------|-------|--------------|-------------|
| WM  | 0   | 7     | 0.9237 | 0.9237 | 0.9266 | 0.9257 | 0.9266 | **0.9267** |
|     |     | 9     | 0.8793 | 0.8786 | 0.8890 | 0.8878 | 0.8890 | **0.8899** |
|     | 20  | 7     | 0.9238 | 0.9238 | 0.9257 | 0.9251 | 0.9261 | **0.9270** |
|     |     | 9     | 0.8798 | 0.8798 | 0.8882 | 0.8879 | 0.8882 | **0.8883** |
|     | 40  | 7     | 0.9045 | 0.9045 | 0.9087 | 0.9076 | 0.9085 | **0.9096** |
|     |     | 9     | 0.8702 | 0.8698 | 0.8786 | 0.8770 | 0.8779 | **0.8811** |
| GM  | 0   | 7     | 0.8655 | 0.8633 | 0.8753 | 0.8745 | **0.8754** | 0.8706 |
|     |     | 9     | 0.8000 | 0.7945 | 0.8251 | 0.8248 | **0.8269** | 0.8188 |
|     | 20  | 7     | 0.8718 | 0.8703 | 0.8782 | 0.8779 | **0.8804** | 0.8766 |
|     |     | 9     | 0.8000 | 0.7962 | 0.8225 | 0.8228 | **0.8263** | 0.8148 |
|     | 40  | 7     | 0.8455 | 0.8440 | 0.8602 | 0.8582 | **0.8614** | 0.8550 |
|     |     | 9     | 0.7912 | 0.7872 | 0.8148 | 0.8141 | **0.8169** | 0.8101 |
| CSF | 0   | 7     | 0.7999 | 0.7967 | **0.8117** | 0.8115 | 0.8085 | 0.8098 |
|     |     | 9     | 0.7533 | 0.7454 | 0.7931 | **0.7962** | 0.7919 | 0.7836 |
|     | 20  | 7     | 0.8231 | 0.8208 | 0.8292 | 0.8303 | 0.8304 | **0.8316** |
|     |     | 9     | 0.7590 | 0.7531 | 0.7983 | **0.8029** | 0.7995 | 0.7888 |
|     | 40  | 7     | 0.8050 | 0.8037 | **0.8309** | 0.8290 | 0.8304 | 0.8242 |
|     |     | 9     | 0.7534 | 0.7480 | 0.7936 | **0.7960** | 0.7937 | 0.7863 |

methods. Tables 10, 11, 12 and 13 show the the performance in terms of *DS*, *JS*, *FNR* and *FPR* for GM on this dataset (The result in boldface shows the best performing method in Tables). The performance of the proposed methods in terms of these measures for GM on average is better than the FCM and other three IFCM methods.

## 5.3 Statistical test

Friedman test, a two way non-parametric statistical test is conducted to find out the significant difference among the proposed and other segmentation methods for both the publicly available datasets. The null hypothesis ($H_0$) of this test is that there is no significant difference in the performance of the proposed and other segmentation methods whereas the alternative hypothesis ($H_1$) defines as the performance of the proposed and other methods are different. For a given performance measure $M$, the $H_0$ and $H_1$ can be defined as:

$$H_0 : \mu_{FCM}^{M} = \mu_{IFCM[8]}^{M} = \mu_{IFCM[35]}^{M} = \mu_{PIFCM}^{M} = \mu_{MIFCM\_Sugeno}^{M} = \mu_{MIFCM\_Yager}^{M}$$
(39)

$$H_1 : \mu_{FCM}^{M} \neq \mu_{IFCM[8]}^{M} \neq \mu_{IFCM[35]}^{M} \neq \mu_{PIFCM}^{M} \neq \mu_{MIFCM\_Sugeno}^{M} \neq \mu_{MIFCM\_Yager}^{M}$$
(40)

where $M \in \{ASA, DS, JS, FNR, FPR\}$. The rank of different segmentation methods, according to the different performance measures is obtained for comparing the methods separately. In Friedman test, the average rank $R_j$ of $j^{th}$ methods for a given $N$ number of images is obtained with respect to a given performance measure as:

$$R_j = \frac{1}{N} \sum_{i=1}^{N} r_i^{j}$$
(41)

**Table 5** Jaccard Score for BrainWeb simulated MRI

|  | INU | Noise | FCM | IFCM [8] | IFCM [35] | PIFCM | MIFCM_Sugeno | MIFCM_Yager |
|---|---|---|---|---|---|---|---|---|
| WM | 0 | 7 | 0.8583 | 0.8583 | 0.8633 | 0.8618 | 0.8633 | **0.8634** |
|  |  | 9 | 0.7845 | 0.7835 | 0.8001 | 0.7983 | 0.8001 | **0.8017** |
|  | 20 | 7 | 0.8584 | 0.8584 | 0.8617 | 0.8607 | 0.8624 | **0.8640** |
|  |  | 9 | 0.7854 | 0.7854 | 0.7989 | 0.7983 | 0.7989 | **0.7990** |
|  | 40 | 7 | 0.8257 | 0.8257 | 0.8327 | 0.8309 | 0.8324 | **0.8342** |
|  |  | 9 | 0.7703 | 0.7695 | 0.7835 | 0.7810 | 0.7823 | **0.7874** |
| GM | 0 | 7 | 0.7630 | 0.7595 | 0.7783 | 0.7771 | **0.7785** | 0.7708 |
|  |  | 9 | 0.6667 | 0.6590 | 0.7023 | 0.7019 | **0.7048** | 0.6931 |
|  | 20 | 7 | 0.7728 | 0.7704 | 0.7829 | 0.7824 | **0.7864** | 0.7803 |
|  |  | 9 | 0.6667 | 0.6614 | 0.6985 | 0.6989 | **0.7040** | 0.6875 |
|  | 40 | 7 | 0.7324 | 0.7301 | 0.7547 | 0.7516 | **0.7565** | 0.7468 |
|  |  | 9 | 0.6546 | 0.6490 | 0.6875 | 0.6865 | **0.6904** | 0.6809 |
| CSF | 0 | 7 | 0.6665 | 0.6621 | **0.6831** | 0.6827 | 0.6785 | 0.6804 |
|  |  | 9 | 0.6042 | 0.5942 | 0.6572 | **0.6614** | 0.6554 | 0.6441 |
|  | 20 | 7 | 0.6994 | 0.6961 | 0.7082 | 0.7099 | 0.7100 | **0.7118** |
|  |  | 9 | 0.6116 | 0.6040 | 0.6643 | **0.6707** | 0.6660 | 0.6512 |
|  | 40 | 7 | 0.6737 | 0.6718 | **0.7107** | 0.7079 | 0.7101 | 0.7010 |
|  |  | 9 | 0.6043 | 0.5974 | 0.6578 | **0.6612** | 0.6580 | 0.6478 |

**Table 6** FNR for BrainWeb simulated MRI

|  | INU | Noise | FCM | IFCM [8] | IFCM [35] | PIFCM | MIFCM_Sugeno | MIFCM_Yager |
|---|---|---|---|---|---|---|---|---|
| WM | 0 | 7 | 0.0885 | 0.0885 | 0.0758 | 0.0802 | 0.0758 | **0.0708** |
|  |  | 9 | 0.1605 | 0.1618 | 0.1308 | 0.1359 | 0.1308 | **0.1252** |
|  | 20 | 7 | 0.0989 | 0.0989 | 0.0875 | 0.0912 | 0.0866 | **0.0815** |
|  |  | 9 | 0.1692 | 0.1692 | 0.1395 | 0.1434 | 0.1404 | **0.1375** |
|  | 40 | 7 | 0.1330 | 0.1330 | 0.1186 | 0.1226 | 0.1193 | **0.1128** |
|  |  | 9 | 0.1847 | 0.1860 | 0.1578 | 0.1631 | 0.1600 | **0.1503** |
| GM | 0 | 7 | 0.1416 | 0.1451 | 0.1294 | 0.1280 | **0.1266** | 0.1452 |
|  |  | 9 | 0.1875 | 0.1955 | 0.1607 | 0.1569 | **0.1553** | 0.1789 |
|  | 20 | 7 | 0.1216 | 0.1238 | 0.1129 | 0.1112 | **0.1079** | 0.1249 |
|  |  | 9 | 0.1829 | 0.1891 | 0.1599 | 0.1565 | **0.1504** | 0.1784 |
|  | 40 | 7 | 0.1363 | 0.1383 | 0.1173 | 0.1180 | **0.1127** | 0.1337 |
|  |  | 9 | 0.1832 | 0.1898 | 0.1572 | 0.1546 | **0.1496** | 0.1743 |
| CSF | 0 | 7 | 0.2431 | **0.2424** | 0.2560 | 0.2486 | 0.2659 | 0.2486 |
|  |  | 9 | 0.2516 | 0.2533 | 0.2543 | **0.2455** | 0.2659 | 0.2547 |
|  | 20 | 7 | **0.2016** | 0.2027 | 0.2193 | 0.2122 | 0.2275 | 0.2091 |
|  |  | 9 | 0.2210 | 0.2227 | 0.2234 | **0.2105** | 0.2360 | 0.2197 |
|  | 40 | 7 | 0.1976 | 0.1976 | 0.2006 | **0.1942** | 0.2098 | 0.1982 |
|  |  | 9 | 0.2329 | 0.2305 | 0.2353 | **0.2251** | 0.2458 | 0.2319 |

**Table 7** FPR for BrainWeb simulated MRI

|  | INU | Noise | FCM | IFCM [8] | IFCM [35] | PIFCM | MIFCM_Sugeno | MIFCM_Yager |
|---|---|---|---|---|---|---|---|---|
| WM | 0 | 7 | **0.0620** | **0.0620** | 0.0706 | 0.0674 | 0.0706 | 0.0762 |
|  |  | 9 | 0.0701 | **0.0698** | 0.0864 | 0.0825 | 0.0864 | 0.0912 |
|  | 20 | 7 | **0.0497** | **0.0497** | 0.0589 | 0.0559 | 0.0592 | 0.0631 |
|  |  | 9 | **0.0578** | **0.0578** | 0.0771 | 0.0730 | 0.0760 | 0.0795 |
|  | 40 | 7 | **0.0501** | **0.0501** | 0.0585 | 0.0560 | 0.0580 | 0.0635 |
|  |  | 9 | 0.0585 | **0.0578** | 0.0748 | 0.0716 | 0.0737 | 0.0791 |
| GM | 0 | 7 | 0.1252 | 0.1256 | 0.1186 | 0.1222 | 0.1219 | **0.1089** |
|  |  | 9 | 0.2187 | 0.2208 | 0.1951 | 0.2012 | 0.1985 | **0.1846** |
|  | 20 | 7 | 0.1367 | 0.1374 | 0.1330 | 0.1360 | 0.1344 | **0.1215** |
|  |  | 9 | 0.2256 | 0.2260 | 0.2028 | 0.2069 | 0.2068 | **0.1952** |
|  | 40 | 7 | 0.1794 | 0.1803 | 0.1696 | 0.1736 | 0.1729 | **0.1600** |
|  |  | 9 | 0.2479 | 0.2484 | 0.2260 | 0.2315 | 0.2317 | **0.2127** |
| CSF | 0 | 7 | 0.1357 | 0.1442 | 0.0891 | 0.1006 | **0.0819** | 0.1044 |
|  |  | 9 | 0.2387 | 0.2567 | 0.1346 | 0.1408 | **0.1200** | 0.1571 |
|  | 20 | 7 | 0.1414 | 0.1455 | 0.1023 | 0.1098 | **0.0881** | 0.1112 |
|  |  | 9 | 0.2737 | 0.2870 | 0.1690 | 0.1772 | **0.1472** | 0.1982 |
|  | 40 | 7 | 0.1911 | 0.1945 | 0.1248 | 0.1384 | **0.1129** | 0.1438 |
|  |  | 9 | 0.2693 | 0.2880 | 0.1625 | 0.1721 | **0.1462** | 0.1857 |

where $r_i^j \in \{1, 2, \ldots, k\}(1 \leq i \leq N, 1 \leq j \leq k)$ is rank value for $i^{th}$ image and $j^{th}$ method. Table 14 shows the average Friedman ranking of different segmentation methods corresponding to ASA for 14 IBSR brain images and 6 BrainWeb brain images used for experiment and other four performance measures evaluated for GM for same set of images [12, 13]. Lowest rank for a segmentation method shows its better performance compared to other methods for a given performance measure. On the basis of Friedman ranking the MIFCM_Sugeno performs better in terms of $ASA$, $DS$, $JS$, $FNR$ except $FPR$. The statistical hypothesis test proposed by Iman and Davenportis is used. The statistic $F_{ID}$ is defined by Iman and Davenport [16] as:

$$F_{ID} = \frac{(N-1)\chi_F^2}{N(k-1) - \chi_F^2} \tag{42}$$

which is distributed according to F-distribution with $k - 1$ and $(k - 1)(N - 1)$ degrees of freedom, where $\chi_F^2$ is the Friedman's statistic defined as $\frac{12N}{k(k+1)} \left[ \sum_j R_j^2 - \frac{k(k+1)^2}{4} \right]$. In our experiments $k = 6$ and $N = 20$. The $p$-values obtained by Iman and Davenport statistic are 5.90E-13, 7.50E-9, 7.50E-9, 3.88E-20 and 1.49E-21 corresponding to the performance

**Table 8** Average computation time (in sec.) taken by different methods

| FCM | IFCM [8] | IFCM [35] | PIFCM | MIFCM_Sugeno | MIFCM_Yager |
|---|---|---|---|---|---|
| 0.68 | 1.39 | 0.40 | 0.68 | 2.06 | 4.21 |

**Table 9**  Average segmentation accuracy for IBSR dataset

| Cases | FCM | IFCM [8] | IFCM [35] | PIFCM | MIFCM_Sugeno | MIFCM_Yager |
|-------|-----|----------|-----------|-------|--------------|-------------|
| 100_23 | 0.7666 | 0.7866 | 0.7396 | 0.7326 | **0.7933** | 0.7735 |
| 110_3 | 0.7713 | **0.7897** | 0.7633 | 0.7456 | 0.7769 | 0.7683 |
| 111_2 | 0.7614 | 0.7722 | 0.7714 | 0.7493 | **0.7816** | 0.7682 |
| 112_2 | 0.7576 | 0.7632 | 0.7686 | 0.7563 | **0.7732** | 0.7578 |
| 11_3 | 0.7859 | 0.7920 | 0.7752 | 0.7635 | **0.7982** | 0.7920 |
| 12_3 | 0.7950 | 0.8007 | 0.8021 | 0.7856 | **0.8138** | 0.7956 |
| 13_3 | 0.8461 | 0.8472 | **0.8485** | 0.8342 | **0.8485** | 0.8419 |
| 17_3 | 0.7188 | 0.7154 | **0.7631** | 0.7324 | 0.7587 | 0.7239 |
| 191_3 | 0.7763 | 0.7792 | 0.7866 | 0.7701 | **0.7969** | 0.7775 |
| 1_24 | 0.7510 | 0.7634 | 0.7699 | 0.7470 | **0.7727** | 0.7593 |
| 202_3 | 0.7784 | 0.7973 | 0.7707 | 0.7475 | **0.8055** | 0.7705 |
| 205_3 | 0.7667 | **0.7780** | 0.7514 | 0.7445 | 0.7730 | 0.7695 |
| 7_8 | 0.6912 | 0.6976 | **0.7401** | 0.7111 | 0.7361 | 0.7034 |
| 8_4 | 0.6462 | 0.6525 | **0.7052** | 0.6711 | 0.7046 | 0.6569 |
| Average | 0.7580 | 0.7668 | 0.7683 | 0.7493 | **0.7809** | 0.7613 |

measures *ASA*, *DS*, *JS*, *FNR* and *FPR* respectively, which advocate the rejection of null hypothesis $H_0$ as there is significant difference among different segmentation methods at the significance level of 0.05. However, these $p$-values so obtained are not suitable for comparison with the control method, i.e. the one that emerges with the lowest rank. So adjusted $p$-values [12] are computed which take into account the error accumulated and provide the correct correlation. This is done with respect to a control method which is the proposed

**Table 10**  DS for IBSR dataset for GM

| Cases | FCM | IFCM [8] | IFCM [35] | PIFCM | MIFCM_Sugeno | MIFCM_Yager |
|-------|-----|----------|-----------|-------|--------------|-------------|
| 100_23 | 0.8191 | **0.8337** | 0.7858 | 0.7887 | 0.8298 | 0.8234 |
| 110_3 | 0.7951 | **0.8123** | 0.7750 | 0.7649 | 0.7887 | 0.7900 |
| 111_2 | 0.7793 | 0.7920 | 0.7832 | 0.7582 | **0.7948** | 0.7862 |
| 112_2 | 0.7729 | 0.7788 | 0.7796 | 0.7648 | **0.7865** | 0.7702 |
| 11_3 | 0.8151 | **0.8187** | 0.7904 | 0.7926 | 0.8122 | **0.8187** |
| 12_3 | 0.8129 | 0.8188 | 0.8145 | 0.8006 | **0.8301** | 0.8125 |
| 13_3 | 0.8564 | **0.8576** | 0.8532 | 0.8398 | 0.8532 | 0.8505 |
| 17_3 | 0.7296 | 0.7291 | 0.7501 | 0.7289 | **0.7530** | 0.7320 |
| 191_3 | 0.7963 | 0.7990 | 0.8030 | 0.7846 | **0.8147** | 0.7955 |
| 1_24 | 0.7481 | 0.7617 | 0.7634 | 0.7336 | **0.7667** | 0.7550 |
| 202_3 | 0.8331 | 0.8489 | 0.8210 | 0.8040 | **0.8529** | 0.8251 |
| 205_3 | 0.8081 | **0.8192** | 0.7867 | 0.7862 | 0.8080 | 0.8104 |
| 7_8 | 0.6800 | 0.6879 | **0.7148** | 0.6873 | 0.7130 | 0.6874 |
| 8_4 | 0.6307 | 0.6403 | 0.6731 | 0.6460 | **0.6743** | 0.6396 |
| Average | 0.7769 | 0.7856 | 0.7781 | 0.7629 | **0.7913** | 0.7783 |

**Table 11** JS for IBSR dataset for GM

| Cases | FCM | IFCM [8] | IFCM [35] | PIFCM | MIFCM_Sugeno | MIFCM_Yager |
|---|---|---|---|---|---|---|
| 100_23 | 0.6937 | **0.7148** | 0.6472 | 0.6511 | 0.7091 | 0.6998 |
| 110_3 | 0.6599 | **0.6839** | 0.6327 | 0.6192 | 0.6511 | 0.6530 |
| 111_2 | 0.6384 | 0.6557 | 0.6436 | 0.6106 | **0.6595** | 0.6478 |
| 112_2 | 0.6299 | 0.6377 | 0.6389 | 0.6192 | **0.6481** | 0.6263 |
| 11_3 | 0.6880 | **0.6930** | 0.6534 | 0.6565 | 0.6838 | **0.6930** |
| 12_3 | 0.6848 | 0.6931 | 0.6870 | 0.6676 | **0.7095** | 0.6842 |
| 13_3 | 0.7488 | **0.7507** | 0.7440 | 0.7239 | 0.7440 | 0.7399 |
| 17_3 | 0.5743 | 0.5737 | 0.6001 | 0.5734 | **0.6038** | 0.5773 |
| 191_3 | 0.6616 | 0.6653 | 0.6709 | 0.6456 | **0.6873** | 0.6604 |
| 1_24 | 0.5975 | 0.6151 | 0.6173 | 0.5792 | **0.6217** | 0.6065 |
| 202_3 | 0.7139 | 0.7375 | 0.6963 | 0.6722 | **0.7436** | 0.7023 |
| 205_3 | 0.6780 | **0.6937** | 0.6484 | 0.6477 | 0.6779 | 0.6812 |
| 7_8 | 0.5152 | 0.5243 | **0.5562** | 0.5236 | 0.5540 | 0.5237 |
| 8_4 | 0.4606 | 0.4709 | 0.5072 | 0.4771 | **0.5086** | 0.4701 |
| Average | 0.6389 | 0.6507 | 0.6388 | 0.6191 | **0.6573** | 0.6404 |

method MIFCM_Sugeno (lowest rank for *ASA*, *DS*, *JS*, *FNR*). For this, a set of post-hoc procedures are defined and adjusted *p*-values are computed. The most widely used post-hoc method [12] to obtain adjusted *p*-values is Holm procedure. Table 15 shows the various value of adjusted *p*-values obtained. From this Table, it is clear that there is statistical difference in terms of *ASA*, *DS*, *JS* and *FNR* between proposed method and other methods except IFCM [35].

**Table 12** FNR for IBSR dataset for GM

| Cases | FCM | IFCM [8] | IFCM [35] | PIFCM | MIFCM_Sugeno | MIFCM_Yager |
|---|---|---|---|---|---|---|
| 100_23 | 0.2631 | 0.2369 | 0.3004 | 0.3082 | **0.2319** | 0.2547 |
| 110_3 | 0.2877 | **0.2575** | 0.3092 | 0.3344 | 0.2875 | 0.2954 |
| 111_2 | 0.2974 | 0.2717 | 0.2924 | 0.3386 | **0.2708** | 0.2852 |
| 112_2 | 0.3260 | 0.3167 | 0.3226 | 0.3479 | **0.3079** | 0.3348 |
| 11_3 | 0.2547 | **0.2460** | 0.2824 | 0.2954 | 0.2465 | **0.2460** |
| 12_3 | 0.2604 | 0.2512 | 0.2621 | 0.2865 | **0.2294** | 0.2633 |
| 13_3 | 0.1728 | **0.1677** | 0.1778 | 0.2155 | 0.1778 | 0.1870 |
| 17_3 | 0.2995 | 0.2934 | 0.2802 | 0.3259 | **0.2598** | 0.2977 |
| 191_3 | 0.3054 | 0.3009 | 0.2999 | 0.3307 | **0.2795** | 0.3104 |
| 1_24 | 0.3379 | 0.3153 | 0.3204 | 0.3719 | **0.3129** | 0.3297 |
| 202_3 | 0.2613 | 0.2334 | 0.2755 | 0.3058 | **0.2260** | 0.2738 |
| 205_3 | 0.2819 | **0.2609** | 0.3059 | 0.3161 | 0.2749 | 0.2781 |
| 7_8 | 0.3929 | 0.3742 | **0.3497** | 0.3982 | **0.3497** | 0.3869 |
| 8_4 | 0.4649 | 0.4487 | 0.3977 | 0.4514 | **0.3948** | 0.4537 |
| Average | 0.3004 | 0.2839 | 0.2983 | 0.3305 | **0.2750** | 0.2997 |

**Table 13** FPR for IBSR dataset for GM

| Cases | FCM | IFCM [8] | IFCM [35] | PIFCM | MIFCM_Sugeno | MIFCM_Yager |
|-------|-----|----------|-----------|-------|--------------|-------------|
| 100_23 | **0.0623** | 0.0676 | 0.0810 | 0.0626 | 0.0832 | 0.0651 |
| 110_3 | 0.0794 | 0.0856 | 0.0919 | **0.0749** | 0.0944 | 0.0791 |
| 111_2 | 0.1007 | 0.1107 | 0.0994 | **0.0832** | 0.1057 | 0.1035 |
| 112_2 | 0.0700 | 0.0716 | 0.0603 | **0.0531** | 0.0678 | 0.0622 |
| 11_3 | 0.0834 | 0.0880 | 0.0983 | **0.0733** | 0.1018 | 0.0880 |
| 12_3 | 0.0800 | 0.0803 | 0.0740 | **0.0688** | 0.0860 | 0.0769 |
| 13_3 | 0.1048 | 0.1086 | 0.1051 | **0.0837** | 0.1051 | 0.0988 |
| 17_3 | 0.2198 | 0.2316 | 0.1994 | **0.1755** | 0.2259 | 0.2166 |
| 191_3 | 0.0499 | 0.0509 | 0.0436 | **0.0367** | 0.0482 | 0.0443 |
| 1_24 | 0.1081 | 0.1132 | 0.1009 | **0.0844** | 0.1053 | 0.1053 |
| 202_3 | 0.0347 | 0.0395 | 0.0404 | **0.0327** | 0.0410 | 0.0341 |
| 205_3 | 0.0591 | 0.0655 | 0.0706 | **0.0559** | 0.0696 | 0.0597 |
| 7_8 | 0.1784 | 0.1936 | 0.1692 | **0.1494** | 0.1738 | 0.1706 |
| 8_4 | 0.1618 | 0.1707 | 0.1873 | **0.1499** | 0.1899 | 0.1621 |
| Average | 0.0995 | 0.1055 | 0.1015 | **0.0846** | 0.1070 | 0.0976 |

**Table 14** Friedman ranking of different methods

| Measures\Methods | MIFCM_Sugeno | IFCM [35] | IFCM [8] | MIFCM_Yager | FCM | PIFCM |
|------------------|--------------|-----------|----------|-------------|-----|-------|
| ASA | 1.35 | 2.5 | 3.875 | 3.925 | 4.7 | 4.65 |
| DS | 1.675 | 3.025 | 3.425 | 3.525 | 4.25 | 5.1 |
| JS | 1.675 | 3.025 | 3.425 | 3.525 | 4.25 | 5.1 |
| FNR | 1.35 | 3.1 | 2.825 | 3.875 | 3.95 | 5.9 |
| FPR | 4.75 | 3.375 | 5.325 | 2.65 | 3.85 | 1.05 |

**Table 15** Adjusted $p$-values (FRIEDMAN)

| | Algorithm | FCM | PIFCM | MIFCM_Yager | IFCM [8] | IFCM [35] |
|---|-----------|-----|-------|-------------|----------|-----------|
| ASA | Unadjusted p | 1.49E-08 | 2.43E-08 | 1.35E-05 | 1.97E-05 | 0.051913 |
| | pHolm | 7.46E-08 | 9.73E-08 | 4.04E-05 | 4.04E-05 | 0.051913 |
| DS | Unadjusted p | 1.35E-05 | 7.07E-09 | 1.77E-03 | 3.10E-03 | 0.022494 |
| | pHolm | 5.38E-05 | 3.53E-08 | 5.30E-03 | 6.19E-03 | 0.022494 |
| JS | Unadjusted p | 1.35E-05 | 7.07E-09 | 1.77E-03 | 3.10E-03 | 0.022494 |
| | pHolm | 5.38E-05 | 3.53E-08 | 5.30E-03 | 6.19E-03 | 0.022494 |
| FNR | Unadjusted p | 1.11E-05 | 1.46E-14 | 1.97E-05 | 0.01266 | 3.10E-03 |
| | pHolm | 4.43E-05 | 7.30E-14 | 5.92E-05 | 0.01266 | 6.19E-03 |

# 6 Conclusion

In this paper, we have proposed modified IFCM for segmentation of brain MRI data to handle uncertainty associated with it due to imprecise measurement and noise. We have solved analytically the optimization problem using Lagrange method of undetermined multiplier. The proposed method is not very sensitive to the parameter in contrast to the earlier similar works. We have performed experiments on a synthetic dataset, BrainWeb dataset and real brain IBSR dataset and compared the performance in terms of quantitative measures (*ASA*, *DS*, *JS*, *FNR* and *FPR*) with the FCM and three variants of IFCM methods. The experimental evidences endorses the efficacy of the proposed method in comparison to the existing methods. We have also performed the Friedman statistical test which shows the superior performance of the proposed method.

**Compliance with Ethical Standards**

**Conflict of interests** The authors declare that they have no conflict of interest.

# Appendix A: Derivation for the membership value and cluster center

The Lagrangian for the objective function (18) can be given as

$$L = \sum_{i=1}^{c} \sum_{j=1}^{N} \left( \frac{(\lambda+1)\mu_{ij}}{1+\lambda\mu_{ij}} \right)^m \|\mathbf{x}_j^{IFS} - \mathbf{v}_i^{IFS}\|^2 + \sum_{j=1}^{N} Y_j (1 - \sum_{i=1}^{c} \mu_{ij}) \quad (43)$$

$$\frac{\partial L}{\partial \mu_{ij}} = m \left( \frac{(\lambda+1)\mu_{ij}}{1+\lambda\mu_{ij}} \right)^{m-1} \left[ \frac{(\lambda+1)}{1+\lambda\mu_{ij}} - \frac{\lambda(\lambda+1)\mu_{ij}}{(1+\lambda\mu_{ij})^2} \right] \left( \|\mathbf{x}_j^{IFS} - \mathbf{v}_i^{IFS}\|^2 \right) - Y_j = 0$$

$$\Rightarrow m \left( \frac{(\lambda+1)}{1+\lambda\mu_{ij}} \right)^m \mu_{ij}^{m-1} \left[ \frac{1}{(1+\lambda\mu_{ij})} \right] \left( \|\mathbf{x}_j^{IFS} - \mathbf{v}_i^{IFS}\|^2 \right) - Y_j = 0$$

$$\Rightarrow \mu_{ij}^{m-1} = \left( \frac{Y_j}{m(\lambda+1)^m} \right) \left[ \frac{(1+\lambda\mu_{ij})^{m+1}}{\left( \|\mathbf{x}_j^{IFS} - \mathbf{v}_i^{IFS}\|^2 \right)} \right]$$

$$\Rightarrow \mu_{ij} = \left( \frac{Y_j}{m(\lambda+1)^m} \right)^{\frac{1}{m-1}} \left[ \frac{(1+\lambda\mu_{ij})^{\frac{m+1}{m-1}}}{\left( \|\mathbf{x}_j^{IFS} - \mathbf{v}_i^{IFS}\|^2 \right)^{\frac{1}{m-1}}} \right]$$

$$\Rightarrow \sum_{i=1}^{c} \mu_{ij} = \sum_{i=1}^{c} \left( \frac{Y_j}{m(\lambda+1)^m} \right)^{\frac{1}{m-1}} \left[ \frac{(1+\lambda\mu_{ij})^{\frac{m+1}{m-1}}}{\left( \|\mathbf{x}_j^{IFS} - \mathbf{v}_i^{IFS}\|^2 \right)^{\frac{1}{m-1}}} \right] = 1$$

$$\Rightarrow \left(\frac{Y_j}{m(\lambda+1)^m}\right)^{\frac{1}{m-1}} = \frac{1}{\sum_{i=1}^{c} \frac{(1+\lambda\mu_{ij})^{\frac{m+1}{m-1}}}{\left(\|\mathbf{x}_j^{IFS}-\mathbf{v}_i^{IFS}\|^2\right)^{\frac{1}{m-1}}}}$$

$$\Rightarrow \mu_{ij} = \frac{\frac{(1+\lambda\mu_{ij})^{\frac{m+1}{m-1}}}{\left(\|\mathbf{x}_j^{IFS}-\mathbf{v}_i^{IFS}\|^2\right)^{\frac{1}{m-1}}}}{\sum_{l=1}^{c} \frac{(1+\lambda u_{lj})^{\frac{m+1}{m-1}}}{\left(\|\mathbf{x}_j^{IFS}-\mathbf{v}_l^{IFS}\|^2\right)^{\frac{1}{m-1}}}}$$

$$\Rightarrow \mu_{ij} = \frac{1}{\sum_{l=1}^{c} \left(\frac{\|\mathbf{x}_j^{IFS}-\mathbf{v}_i^{IFS}\|}{\|\mathbf{x}_j^{IFS}-\mathbf{v}_l^{IFS}\|}\right)^{\frac{2}{m-1}} \left(\frac{1+\lambda u_{lj}}{1+\lambda\mu_{ij}}\right)^{\frac{m+1}{m-1}}} \tag{44}$$

$$\frac{\partial L}{\partial \mu_V(v_i)} = \sum_{j=1}^{N} \left(\frac{(\lambda+1)\mu_{ij}}{1+\lambda\mu_{ij}}\right)^m (\mu_X(x_j)-\mu_V(v_i)) = 0 \tag{45}$$

$$\Rightarrow \sum_{j=1}^{N} \left(\frac{(\lambda+1)\mu_{ij}}{1+\lambda\mu_{ij}}\right)^m \mu_X(x_j) - \sum_{j=1}^{N} \left(\frac{(\lambda+1)\mu_{ij}}{1+\lambda\mu_{ij}}\right)^m \mu_V(v_i) = 0$$

$$\Rightarrow \mu_V(v_i) = \frac{\sum_{j=1}^{N} \left(\frac{(\lambda+1)\mu_{ij}}{1+\lambda\mu_{ij}}\right)^m \mu_X(x_j)}{\sum_{j=1}^{N} \left(\frac{(\lambda+1)\mu_{ij}}{1+\lambda\mu_{ij}}\right)^m} \tag{46}$$

$$\frac{\partial L}{\partial v_V(v_i)} = \sum_{j=1}^{N} \left(\frac{(\lambda+1)\mu_{ij}}{1+\lambda\mu_{ij}}\right)^m (v_X(x_j)-v_V(v_i)) = 0 \tag{47}$$

$$\Rightarrow \sum_{j=1}^{N} \left(\frac{(\lambda+1)\mu_{ij}}{1+\lambda\mu_{ij}}\right)^m v_X(x_j) - \sum_{j=1}^{N} \left(\frac{(\lambda+1)\mu_{ij}}{1+\lambda\mu_{ij}}\right)^m v_V(v_i) = 0$$

$$\Rightarrow v_V(v_i) = \frac{\sum_{j=1}^{N} \left(\frac{(\lambda+1)\mu_{ij}}{1+\lambda\mu_{ij}}\right)^m v_X(x_j)}{\sum_{j=1}^{N} \left(\frac{(\lambda+1)\mu_{ij}}{1+\lambda\mu_{ij}}\right)^m} \tag{48}$$

$$\frac{\partial L}{\partial \pi_V(v_i)} = \sum_{j=1}^{N} \left(\frac{(\lambda+1)\mu_{ij}}{1+\lambda\mu_{ij}}\right)^m (\pi_X(x_j)-\pi_V(v_i)) = 0 \tag{49}$$

$$\Rightarrow \sum_{j=1}^{N} \left(\frac{(\lambda+1)\mu_{ij}}{1+\lambda\mu_{ij}}\right)^m \pi_X(x_j) - \sum_{j=1}^{N} \left(\frac{(\lambda+1)\mu_{ij}}{1+\lambda\mu_{ij}}\right)^m \pi_V(v_i) = 0$$

$$\Rightarrow \pi_V(v_i) = \frac{\sum_{j=1}^{N} \left(\frac{(\lambda+1)\mu_{ij}}{1+\lambda\mu_{ij}}\right)^m \pi_X(x_j)}{\sum_{j=1}^{N} \left(\frac{(\lambda+1)\mu_{ij}}{1+\lambda\mu_{ij}}\right)^m} \tag{50}$$

# References

1. Alipour S, Shanbehzadeh J (2014) Fast automatic medical image segmentation based on spatial kernel fuzzy c-means on level set method. Mach Vis Appl 25(6):1469–1488
2. Atanassov KT (1986) Intuitionistic fuzzy sets. Fuzzy Sets Syst 20(1):87–96

3. Atanassov KT (2003) Intuitionistic fuzzy sets: past, present and future. In: EUSFLAT conference, pp 12–19
4. Balafar MA, Ramli AR, Saripan MI, Mashohor S (2010) Review of brain mri image segmentation methods. Artif Intell Rev 33(3):261–274
5. Benaichouche A, Oulhadj H, Siarry P (2013) Improved spatial fuzzy c-means clustering for image segmentation using pso initialization, mahalanobis distance and post-segmentation correction. Digital Signal Process 23(5):1390–1400
6. Bezdek JC (1981) Objective Function Clustering. In: Pattern recognition with fuzzy objective function algorithms. Springer, pp 43–93
7. Bustince H, Kacprzyk J, Mohedano V (2000) Intuitionistic fuzzy generators application to intuitionistic fuzzy complementation. Fuzzy Sets Syst 114(3):485–504
8. Chaira T (2011) A novel intuitionistic fuzzy c means clustering algorithm and its application to medical images. Appl Soft Comput 11(2):1711–1717
9. Chen X, Nguyen BP, Chui CK, Ong SH (2016) Automated brain tumor segmentation using kernel dictionary learning and superpixel-level features. In: 2016 IEEE international conference on systems, man, and cybernetics (SMC). IEEE, pp 002,547–002,552
10. Chuang KS, Tzeng HL, Chen S, Wu J, Chen TJ (2006) Fuzzy c-means clustering with spatial information for image segmentation. Comput Med Imaging Graph 30(1):9–15
11. Cocosco CA, Kollokian V, Kwan RKS, Pike GB, Evans AC (1997) Brainweb: online interface to a 3d mri simulated brain database. In: NeuroImage. Citeseer
12. Derrac J, García S, Molina D, Herrera F (2011) A practical tutorial on the use of nonparametric statistical tests as a methodology for comparing evolutionary and swarm intelligence algorithms. Swarm Evol Comput 1(1):3–18
13. Friedman M (1937) The use of ranks to avoid the assumption of normality implicit in the analysis of variance. J Am Stat Assoc 32(200):675–701
14. Huang CW, Lin KP, Wu MC, Hung KC, Liu GS, Jen CH (2015) Intuitionistic fuzzy c-means clustering algorithm with neighborhood attraction in segmenting medical image. Soft Comput 19(2):459–470
15. Iakovidis D, Pelekis N, Kotsifakos E, Kopanakis I (2008) Intuitionistic fuzzy clustering with applications in computer vision. In: Advanced concepts for intelligent vision systems. Springer, pp 764–774
16. Iman RL, Davenport JM (1980) Approximations of the critical region of the fbietkan statistic. Communications in Statistics-Theory and Methods 9(6):571–595
17. Ji ZX, Sun QS, Xia DS (2014) A framework with modified fast fcm for brain mr images segmentation (retraction of vol 44, pg 999, 2011). Pattern Recogn 47(12):3979–3979
18. Kannan S, Devi R, Ramathilagam S, Takezawa K (2013) Effective fcm noise clustering algorithms in medical images. Comput Biol Med 43(2):73–83
19. Krinidis S, Chatzis V (2010) A robust fuzzy local information c-means clustering algorithm. IEEE Trans Image Process 19(5):1328–1337
20. Krishnapuram R, Keller JM (1993) A possibilistic approach to clustering. IEEE Trans Fuzzy Syst 1(2):98–110
21. Li C, Huang R, Ding Z, Gatenby JC, Metaxas DN, Gore JC (2011) A level set method for image segmentation in the presence of intensity inhomogeneities with application to mri. IEEE Trans Image Process 20(7):2007–2016
22. Murofushi T, Sugeno M (2000) Fuzzy measures and fuzzy integrals. In: Fuzzy measures and integrals: theory and applications, pp 3–41
23. Olabarriaga SD, Smeulders AW (2001) Interaction in the segmentation of medical images: a survey. Med Image Anal 5(2):127–142
24. Pelekis N, Iakovidis DK, Kotsifakos EE, Kopanakis I (2008) Fuzzy clustering of intuitionistic fuzzy data. International Journal of Business Intelligence and Data Mining 3(1):45–65
25. Pham DL, Xu C, Prince JL (2000) Current methods in medical image segmentation 1. Annu Rev Biomed Eng 2(1):315–337
26. Qiu C, Xiao J, Yu L, Han L, Iqbal MN (2013) A modified interval type-2 fuzzy c-means algorithm with application in mr image segmentation. Pattern Recogn Lett 34(12):1329–1338
27. Sato M, Lakare S, Wan M, Kaufman A, Nakajima M (2000) A gradient magnitude based region growing algorithm for accurate segmentation. In: 2000 international conference on image processing, 2000. Proceedings, vol 3. IEEE, pp 448–451
28. Szmidt E, Kacprzyk J (2000) Distances between intuitionistic fuzzy sets. Fuzzy Sets Syst 114(3):505–518
29. Verma H, Agrawal R (2015) Possibilistic intuitionistic fuzzy c-means clustering algorithm for mri brain image segmentation. Int J Artif Intell Tools 24(05):1550,016
30. Verma H, Agrawal R, Sharan A (2016) An improved intuitionistic fuzzy c-means clustering algorithm incorporating local information for brain image segmentation. Appl Soft Comput 46:543–557

31. Vlachos IK, Sergiadis GD (2007) The role of entropy in intuitionistic fuzzy contrast enhancement. In: International fuzzy systems association world congress. Springer, pp 104–113
32. Vovk U, Pernus F, Likar B (2007) A review of methods for correction of intensity inhomogeneity in mri. IEEE Trans Med Imaging 26(3):405–421
33. Wang L, Chen Y, Pan X, Hong X, Xia D (2010) Level set segmentation of brain magnetic resonance images based on local gaussian distribution fitting energy. J Neurosci Methods 188(2):316–325
34. Wang Z, Song Q, Soh YC, Sim K (2013) An adaptive spatial information-theoretic fuzzy clustering algorithm for image segmentation. Comput Vis Image Underst 117(10):1412–1420
35. Xu Z, Wu J (2010) Intuitionistic fuzzy c-means clustering algorithms. J Syst Eng Electron 21(4):580–590
36. Yager RR (1979) On the measure of fuzziness and negation part i: membership in the unit interval. Int J Gen Syst 5(4):221–229
37. Yager RR (1980) On the measure of fuzziness and negation. II. Lattices. Inf Control 44(3):236–260
38. Zadeh LA (1965) Fuzzy sets. Inf Control 8(3):338–353

**Mr. Dhirendra Kumar** is Ph.D research scholar from Jawaharlal Nehru University, New Delhi. He received his B.Sc. degree from Banaras Hindu University, Varanasi, year 2011. He had completed M.Sc. in computer science from the same university in the year 2013. He has done M. Tech. in Computer Science and Technology from Jawaharlal Nehru University in year 2015. His research interest is medical image segmentation, pattern recognition, image classification.



**Dr. Hanuman Verma** has completed his Ph. D from Jawaharlal Nehru University, New Delhi, India in 2015. He also received M. Tech in Computer Science and Technology from Jawaharlal Nehru University, New Delhi, India in 2010. He has published research papers in reputed International Journals and Conferences including Elsevier, Wiley, World Scientific, and Springer. His primary research interest includes Clustering algorithms, Fuzzy set theory, Soft computing, Image segmentation, and Applied mathematics.

**Dr. Aparna Mehra** is Associate Professor in Department of Mathematics, Indian Institute of Technology, New Delhi. She received her Ph.D in Mathematics, from University of Delhi, Delhi. Her research interest includes Optimization Theory, Variational Inequalities, Matrix Games Optimization, Fuzzy Optimization, Portfolio Optimization & Management, Bipolar Fuzzy Set Theory. She has published many research papers in reputed International Journals and conferences.



**Prof. R. K. Agrawal** received M.Tech (Computer Application) from Indian Institute of Technology Delhi, New Delhi and Ph. D (Computational Physics) from University of Delhi, Delhi. Presently, he is working as Professor at the School of Computer and Systems Sciences, Jawaharlal Nehru University, New Delhi. He has published many research papers in reputed International Journals. His research areas are Data Mining, Pattern Recognition and Security.